

# Gender Classification from Iris Images using Fusion of Uniform Local Binary Patterns

Juan E. Tapia<sup>1</sup>, Claudio A. Perez and Kevin W. Bowyer<sup>2</sup>

<sup>1</sup> Department of Electrical Engineering and  
Advanced Mining Technology Center, Universidad de Chile  
jtapiafarias, clperez@ing.uchile.cl,

<sup>2</sup> Department of Computer Science and Engineering, University of Notre Dame  
kwb@nd.edu

**Abstract.** This paper is concerned in analyzing iris texture in order to determine “soft biometric”, attributes of a person, rather than identity. In particular, this paper is concerned with predicting the gender of a person based on analysis of features of the iris texture. Previous researchers have explored various approaches for predicting the gender of a person based on iris texture. We explore using different implementations of Local Binary Patterns from the iris image using the masked information. Uniform LBP with concatenated histograms significantly improves accuracy of gender prediction relative to using the whole iris image. Using a subject-disjoint test set, we are able to achieve over 91% correct gender prediction using the texture of the iris. To our knowledge, this is the highest accuracy yet achieved for predicting gender from iris texture.

**Keywords:** Biometrics, Iris, LBP, Gender classification.

## 1 Introduction

Whenever people log onto computers, access an ATM, pass through airport security, use credit cards, or enter high-security areas, they need to verify their identities [1]. Thus, there is tremendous interest in improved methods for reliable and secure identification of people. Gender classification based on iris images is currently one of the most challenging problems in image analysis research [2, 3]. In a biometric recognition framework, gender classification can help by requiring a search of only half of the subjects in the database [4].

One active area of soft biometric research involves classifying the gender of the person from the biometric sample. Most work done on gender classification has involved the analysis of face images and uses Local Binary Patterns (LBP) to increase the accuracy of the identification task [5]. Various types of classifiers have been used in gender classification after feature extraction and selection. Gender recognition is a fundamental task for human beings, as many social functions critically depend on the correct gender perception. Automatic gender classification has many important applications, for example, intelligent user interface, visual surveillance, collecting demographic statistics for marketing, etc. Human faces provides important visual information for gender classification.

Gender classification from face images has received much research interest in the last two decades. Moghaddam and Yang [6] were the first to report the SVM with the Radial Basic Function kernel (SVM+RBF) as the best gender classifier. More recently, Makinen and Raisano [7] compared the performance of SVM with other classifiers including neural networks and Adaboost. According to their published results, SVM achieved the highest performance. In [4, 8] was reported the extension of the use of feature selection based on mutual information and features fusion to improve gender classification of face images. The authors compare the results of fusing 3 groups of features, 3 spatial scales and 4 different mutual information measures to select features. They also showed improved results by fusion of LBP features with different radii and spatial scales, and the selection of features using mutual information.

Gender classification using iris information is a rather new topic, with only a few papers published [9, 2, 3]. Most gender classification methods reported in the literature use all iris texture features for classification or periocular images [10, 11] and using LBP for identification. As a result, gender-irrelevant information might be fed into the classifier which may result in poor generalization, especially when the training set is small. It has been shown both theoretically and empirically that reducing the number of irrelevant or redundant features increases the learning efficiency of the classifier [12].

Thomas et al. [3] were the first to explore gender-from-iris, using images acquired with an LG 2200 sensor. They segmented the iris region, created a normalized iris image, and then a log-Gabor filtered version of the normalized image. In addition to the log-Gabor texture features, they used seven geometric features of the pupil and iris, and were able to reach a gender-prediction accuracy close to 80%.

Lagree et al. [2] experimented with iris images acquired using an LG 4000 sensor. Their work differs from Thomas [3] in several ways. They computed texture features separately for eight five-pixel horizontal bands, running from the pupil-iris boundary out to the iris sclera boundary, and ten twenty-four-pixel vertical bands from a 40x240 image. The normalized image is not processed by the log-Gabor filters that are used by IrisBEE software [13] to create the “iris code” for recognition purpose and no geometrics features are used. This approach reached an accuracy close to 62% for gender and close to 80% for ethnicity.

Bansal et al. [9] experimented with iris images acquired with a Cross Match SCAN-2 dual-iris camera. A statistical feature extraction technique based on correlation between adjacent pixels was combined with a 2D wavelet tree based on feature extraction techniques to extract significant features from the iris image. This approach reached an accuracy of 83.06% for gender classification. Nevertheless, the database used in this experiment was very small (300 images) compared to other studies published in the literature.

Actually numerous variants of LBP descriptors have been proposed in the last years [14–17]. Several works only utilized the uniform patterns but combining uniform patterns with a few non-uniform patterns was shown to improve performance [18, 19].

In this paper we propose a new method to extract information from the iris image to improve gender classification. We first extract texture information in details using small windows and then concatenate the histogram information. Results indicate that each window contains useful information for gender classification. We also consider using overlapping windows, in order to obtaining a more representative histogram. Results indicate that using a subset of the iris region gives greater accuracy than using only the whole iris region. We then explore different implementations using traditional LBP, uniform histogram and concatenated histogram of overlapped windows. We are able to achieve over 91% correct gender classification with the Uniform LBP(8,1).

## 2 Methods

The iris feature extraction process involves the following steps. First, a camera acquires an image of the eye. All commercial iris recognition systems use near-infrared illumination, to be able to image iris texture of both dark and light eyes. Next, the iris region is located within the image. The annular region of the iris is transformed from raw image coordinates to normalized polar coordinates. This results in what is sometimes called an unwrapped or rectangular iris image. A texture filter is applied at a grid of locations on this unwrapped iris image, and the filter responses are quantized to yield a binary iris code [1]. Iris recognition systems operating on these principles are widely used in a variety of applications around the world.

The radial resolution ( $r$ ) and angular resolution ( $\theta$ ) used during the normalization or unwrapping stage determine the size of the rectangular iris image, and can significantly influence the iris recognition rate. This unwrapping is referred to as using Daugman’s rubber sheet model [20]. In this work we use a rectangular image of 20 ( $r$ ) x 240 ( $\theta$ ), created using IrisBEE implementation, as illustrated in Figure 1.

The implementation also creates a segmentation mask of the same size as the rectangular image, masked by default 25% of fragile bits [21]. When using fragile bit masking, we mask a significant amount of information because it is not “stable”. Rather than completely ignoring all of the fragile bits of information, we would like to find a different way of use those bits. We know that the values (zero/one) of those bits are not stable. However, the physical locations of those bits should be stable and might be used to improve our gender classification performance.

The segmentation mask indicates the portions of the normalized iris image that are not valid due to occlusion by eyelids, eyelashes or specular reflections (See, Figure 2.)

For the encoding stage, the output of the Gabor filters is transformed into the binary iris code by quantizing the phase information into four levels, for each possible quadrant in the complex plane. In coding only the phase information, the iris code keep only the most stable information of the iris, while discarding

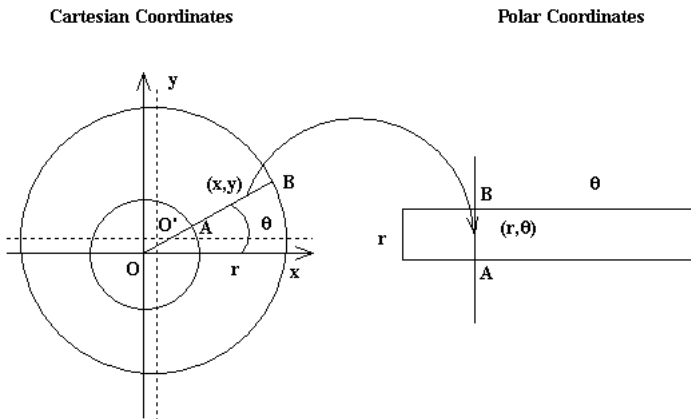


**Fig. 1.** Transformation of Cartesian coordinates  $(x, y)$  to Polar coordinate  $(r, \theta)$  for generating the Unwrapper image.

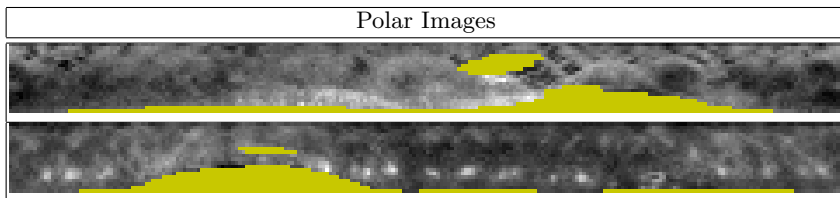


**Fig. 2.** Representation of polar image from the segmented iris region. The iris region is unwrapped to a rectangular image. The segmented areas of iris occlusion are shown in yellow.

redundant or noisy information, which is represented by the amplitude component [20].

The points at which the filter is applied can be viewed as sampling at increments along the radial distance between the pupil-iris boundary and the iris-sclera boundary and at increments of angular distance around the iris. At each point that the filter is applied, a complex-valued result is obtained. The real part and the imaginary part of each result are each quantized to 0/1, giving two bits of iris code for each texture filter result.

Liu et al. [13] have collected a large data set of iris images, intentionally sampling a range of quality broader than that used by current commercial iris recognition systems. The author re-implemented the Daugman-like iris recognition algorithm developed by Masek [22] and also developed and implemented an improved iris segmentation and eyelid detection stage of the algorithm called Iris-BEE, and experimentally verified the improvement in recognition performance using the collected dataset. Compared to Masek's original segmentation approach, this improved segmentation algorithm leads to an increase of over 6% in the rank-one recognition rate.

Figure 3 shows examples of the original image for the left eye with the corresponding segmentation and unwrapped image.

In this research, iris images were divided into 48 sub-regions, using windows size of 10x10 without overlapping and 59 bins for the LBP histogram. The  $LBP(8,1.u2)$  operator was adopted to extract LBP features.

The aim of this work is to find the best way for describing a given texture using a local binary pattern (LBP). First, several different approaches are compared, then the best fusion approach is tested and compared with several approaches proposed in the literature.

An SVM classifier with Gaussian kernel was trained using a LIBSVM implementation [23] with ten fold cross-validation procedure.

## 2.1 Local Binary Patterns (LBP)

LBP is a gray-scale texture operator which characterizes the spatial structure of the local image texture. Given a central pixel in the image, a binary pattern number is computed by comparing its value with those of its neighbors. The original operator used a 3x3 windows size. LBP features were computed from relative pixels intensities in a neighborhood.

$$LBP_{P,R}(x,y) = \bigcup_{(x',y') \in N(x,y)} h(I(x,y), I(x',y')) \quad (1)$$

where  $N(x,y)$  is vicinity around  $(x,y)$ ,  $\cup$  is the concatenation operator,  $P$  is number of neighbors and  $R$  is the radius of the neighborhood.

LBP was first introduced in [14] showing high discriminative power in distinguishing texture features, and is widely used for face analysis. As the neighborhood consists of 8 pixels, a total of  $2^8 = 256$  different labels can be obtained depending on the relative gray values of the center and the pixels in the neighborhood (See, Figure 4.)

Later, in [17] the uniform local binary pattern (ULBP) was introduced, extending the original LBP operator to circular neighborhood with a different radius size and a small subset of LBP patterns selected. A uniformity measure of a pattern is used:  $U$  ("pattern") is the number of bitwise transitions from 0 to 1 or vice versa when the bit pattern is considered circular. A local binary pattern is called uniform if its uniformity measure is at most 2. For example, the patterns 00000000 (0 transitions), 01110000 (2 transitions) and 11001111 (2 transitions) are uniform whereas the patterns 11001001 (4 transitions) and 01010011 (5 transitions) are not. In uniform LBP mapping there is a separate output label for each uniform pattern and all the non-uniform patterns are assigned to a single label. Thus, the number of different output labels for mapping for patterns of  $P$  bits is  $P(P-1) + 3$ . For instance, the uniform mapping produces 59 output labels for neighborhoods of 8 sampling points, and 243 labels for neighborhoods of 16 sampling points.

The reasons for omitting the non-uniform patterns are twofold. First, most of the local binary patterns in natural images are uniform. It was noticed experimentally in [14] that uniform patterns account for a bit less than 90% of all

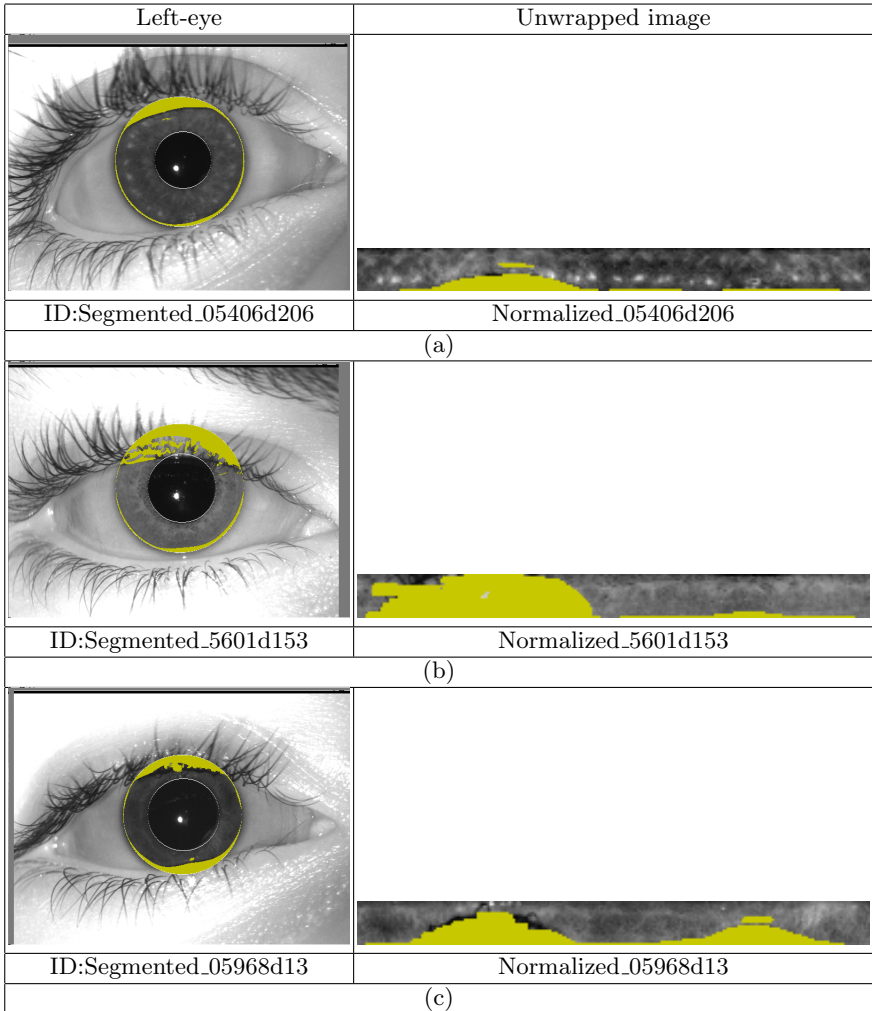


**Fig. 3.** Original images of the left eye from a female subject with eyelids and eyelashes detection using IrisBEE implementation. The Images (a), (b) and (c) represent segmented and normalized image.

patterns when using the (8, 1) neighborhood. In experiments with facial images, it was found that 90.6% of the patterns in the (8, 1) neighborhood and 85.2% of the patterns in the (8, 2) neighborhood are uniform. The second reason for considering uniform patterns is the statistical robustness. Using uniform patterns instead of all the possible patterns has produced better recognition results in many applications [4, 19]. On one hand, there are indications that uniform patterns themselves are more stable, i.e. less prone to noise and on the other hand, considering only uniform patterns makes the number of possible LBP labels significantly lower and reliable estimation of their distribution requires fewer samples.

Rotation invariant patterns have been explored in [16], where patterns that represent 80% of all the patterns in training data are used. The uniform patterns allows to see the LBP method as a unifying approach to the traditionally divergent statistical and structural models of texture analysis.

In [17], was proposed CLBP using both the sign and magnitude information in the difference  $d$  between the central pixel,  $q_c$ , and some pixel in its neighborhood  $q_p$ .

In conventional LBP operator only the sign component of  $d$  is utilized. If  $d_p = q_p - q_c$  its sign  $h$  is as we see above in Eq. (1),  $h(d_p) = 1$  if  $d_p \geq 0$ , otherwise 0. CLBP utilizes the magnitude  $m_p$  of  $d_p$ , where  $m_p = \|d_p\|$ , for additional discriminant power. CLBP also considers the intensity of the central pixel,  $q_c$ . Thus, three operators are defined in CLBP:

CLBP\_S, which considers the sign component of the difference, CLBP\_M, which considers the magnitude component of the difference, and CLBP\_C, which considers the intensity of the central pixel.

CLBP\_S is the conventional LBP sign operator  $h(x)$ .

CLBP\_M is defined as follows:

$$CLBP_{M_{P,R}} = \sum_{p=0}^{P-1} t(m_p, c) 2^p \quad (2)$$

Where  $t(x) = 1$  if  $x \geq 0$ , otherwise 0, and  $c$  is the mean value of absolute value of the differences between a pixel and one neighbor.

CLBP\_C is defined as follow:

$$CLBP_{C_{P,R}} = t(q_p - \tau_1) \quad (3)$$

where  $t(x)$  is defined as in Eq.(2) and  $\tau_1$  is the average gray level of entire image. These three codes are then combined to form CLBP feature map of the original image.

In [15] was proposed Local Binary Pattern Histogram Fourier features (LBP-HF), a novel rotation invariant image descriptor computed from discrete Fourier transforms of local binary pattern (LBP) histograms. Unlike most other histogram based invariant texture descriptors which normalize rotation locally, the proposed invariants are constructed globally for the whole region to be described.

In addition to being rotation invariant, the LBP-HF features retain the highly discriminative nature of LBP histograms.

## 2.2 Dataset

The images used in this paper were taken with an LG 4000 sensor. The LG 4000 uses near-infrared illumination and acquires a 480x640, 8-bit/pixel image. Example LG 4000 iris images appear in Figures 5. We used the UND iris database to train and test a gender classifier. The image dataset for this work consists of one left eye image and one right eye image for each of 750 males and 750 females, for a total of 3,000 images. This dataset is available to other researcher. Additional details and the release agreement are available at: [http://www3.nd.edu/~cvrl/CVRL/Data\\_Sets.html](http://www3.nd.edu/~cvrl/CVRL/Data_Sets.html).

For each subject, one left eye image was selected at random from their set of left eye images, and one right eye image was selected at random from their right eye images.

A training portion of the dataset was created by randomly selecting 80% of the males and 80% of the females, and the images for the remaining 20% of males and 20% of females was set aside as the test portion.

In this paper, experiments are conducted separately for the left eye and the right eye. This reflects the fact that historically many iris recognition applications use an image from only one eye rather than from both eyes. Because the left eye image and the right eye image for a given subject were generally not acquired in the same session, there may be differences in illumination, eyelid occlusion, or pose between the left and right eye images of a person. (For example, see Figure 5.)

## 2.3 Experiments

In this paper, we present different experiments for gender classification from the iris image. A significant limitation of the original LBP operator is its small spatial support area. Features calculated in a local 3x3 neighborhood cannot capture large-scale structures that may be the dominant features of some textures. A straightforward way of enlarging the spatial support area is to combine the information provided by  $N$  LBP operators with varying windows size. This way, each pixel in an image gets  $N$  different LBP codes. The most accurate information would be obtained by using the joint distribution of these codes.

The first approach that we explore is based on histogram of LBP features (LBPH) using uniform features  $ULBP(8,1)$ , where we use 48 windows with size of 10x10 pixels. This represents two vertical regions each with 24 horizontal regions without overlap between regions and concatenated histograms. This approach results in the feature vector for an image having 2,582 values (2 vertical regions x 24 horizontal regions x 59 bins=2,582).

In the second approach, we use the same size of windows but using overlapping of 50%. This way more sub-windows over iris images could be obtained

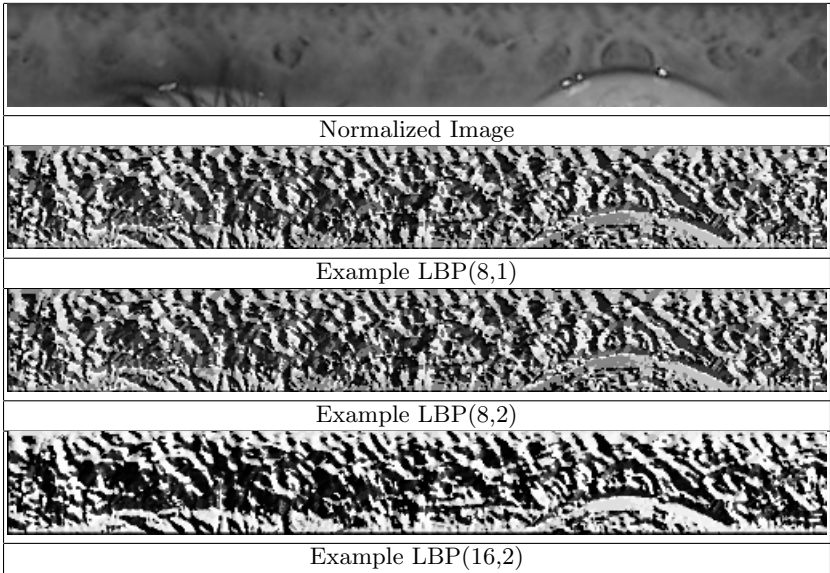


**Fig. 4.** Normalized iris image from segmentation stage and different LBP examples

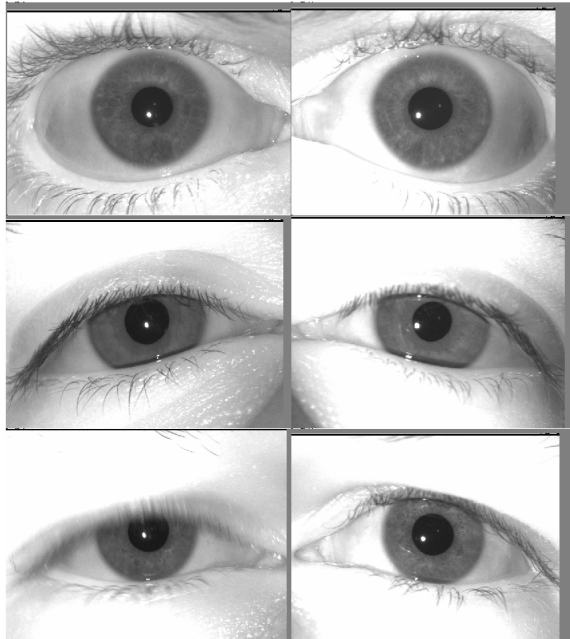


**Fig. 5.** Sample images showing right and left eye images. The image belong to the same person and shows the different illumination level for each eye.

from each image (4 vertical regions x 48 horizontal region x 59 bins=11,328). Each pixel is labeled with the code of the texture primitive that best matches the local neighborhood. Thus each LBP code can be regarded as a micro-texton. Local primitives detected by the LBP include spots, flat areas, edges, edge ends, curves.

### 3 Results

Table I shows the gender classification rate (and standard deviation) obtained using different LBP implementations with the set of the left iris images. The first column identifies the LBP implementation. The second column lists the classification rate, which is also broken down by gender in columns 3 and 4.

The top row of Table I shows the gender classification accuracy obtained using the intensity values of the whole polar image (20x240), without any texture features extracted. The accuracy is 78.52% +/- 1.70.

The second row of Table I shows the classification accuracy using the traditional uniform LBP over the entire image, without overlapping and windows. The accuracy actually decreases substantially compared to using no feature extraction. Accuracy using LBP from this feature extraction method reaches about 71.33% +/- 0.80.

The third row of Table I shows the classification accuracy achieved using the Complete LBP using only the magnitude, over the entire image. The accuracy in this case decreases over that ULBP, reaching only 65.33% +/- 0.90.

The fourth row of Table I shows the classification accuracy achieved using the Complete LBP using only the sign, over the entire image. The accuracy in this case decreases over that ULBP and CLBP-Mag, reaching only 60.33% +/- 0.80.

The fifth and sixth rows of Table I show the classification accuracy achieved using the Complete uniform LBP using the magnitude and sign respectively, over the entire image. The accuracy in this case increases over that previous implementation, reaching 81.33% +/- 0.50 and 77.33% +/- 0.50 respectively.

The seventh row of Table I shows the classification accuracy achieved using the LBP-fourier (8,1), over the entire image. The accuracy in this case reach only 68.33% +/- 0.70.

The eighth row of Table I shows the classification accuracy achieved using the LBP-fourier (16,2), over the entire image. The accuracy in this case reach only 62.33% +/- 0.67.

The best results were obtained for the Uniform LBP (8,1) using windows of size 10x10 pixels without overlapping and Uniform LBP (8,1) with overlapping of the 50% reaching 90.33% +/- 0.35 and 91.33% +/- 0.40 respectively. These result are better than previously published.

It is important to notice that the highest gender classification rates were reached using the overlapping histograms. It may be that small windows contain more specific information for gender classification, or it may be that the

**Table 1.** Gender Classification rate using different LBP implementation. In the first columns see the implementation methods and the second columns the classification rate for the left iris. Columns 3rd and 4 rd show the results by gender.

Implementation	Left eye (%)	Male (%)	Female (%)
Raw Image	78.52 +/- 1.70	77.50	79.53
LBP(8,1)	71.33 +/- 0.80	70.00	73.16
ULBP(8,1)	77.33 +/- 0.70	74.33	80.30
C-LBP-Mag(8,1)	65.33 +/- 0.90	68.25	62.35
C-LBP-Sign (8,1)	60.33 +/- 0.80	58.30	62.33
C-ULBP-Mag(8,1)	81.33 +/- 0.50	84.00	80.00
C-ULBP-Sign (8,1)	77.33 +/- 0.50	76.13	78.66
LBP-Fourier(8,1)	68.33 +/- 0.67	69.50	67.10
LBP-Fourier(16,2)	62.33 +/- 0.35	59.00	65.66
ULBPh(8,1)	90.33 +/- 0.35	92.67	88.00
<b>ULBPh_ov(8,1)</b>	<b>91.33 +/- 0.40</b>	<b>96.67</b>	<b>86.00</b>

information extracted from those windows is more exact due to segmentation accuracies and fusion of histograms.

For the best results in Table I, using the ULBPh\_ov(8,1) selection, the correct classification rate is substantially better for males than for females. For the left eye, the correct classification rate is 96.67% for males, versus 86% for females. This represents 145 correct male images out of 150, and 129 correct female images out of 150. For the second best method ULBPh(8,1), the correct classification rate for males is 92.67% versus 88% for females. This represents 139 correct male images out of 150, and 132 correct female images out of 150.

## 4 Conclusions

This paper is the first to explore uniform LBP using fusion of histograms for predicting gender from the iris image using the polar representation.

The combination of the structural and statistical approaches stems from the fact that the distribution of micro-textons can be seen as statistical placement rules. The LBP distribution therefore has both of the properties of a structural analysis method: texture primitives and placement rules. On the other hand, the distribution is just a statistic of a non-linearly filtered image, clearly making the method a statistical one. For these reasons, the LBP distribution can be successfully used in gender classification using a wide variety of different textures, to which statistical and structural methods have normally been applied separately.

We found very large variations in accuracy based on using different implementations of LBP. The previous results motivate exploring more LBP implementation with different windows size and radii. Of the alternatives considered here, we found that using overlapping windows for histogram LBP(8,1) gave the best accuracy, obtaining 91.33%. This level of accuracy exceeds that of any other publication that we are aware of.

Several steps can be pursued to obtain even better accuracy in gender prediction from iris. We used the IrisBEE implementation in this work, and it is known to have as accurate of iris region segmentation as some other available implementations. Improving the accuracy of the iris region segmentation should naturally improve the accuracy of gender prediction. In this preliminary paper, we have presented results for only the left iris, we are still working on the results of the right iris and the fusion of the information from both irises. Older iris scanners (e.g., the LG 2200) and applications typically used just one iris, either the left or right. But more modern sensors (e.g., the LG 4000) acquire both iris images, and so it makes sense to consider gender prediction based on the combination of left and right polar images.

## 5 Acknowledgements

Thanks to Vince Thomas, Mike Batanian, Steve Lagree and Yingjie Gu for the work they have previously done in this research topic.

## References

1. Bowyer, K.W., Hollingsworth, K., Flynn, P.J.: Image understanding for iris biometrics: A survey. *Computer Vision and Image Understanding* **110**(2) (2008) 281–307
2. Lagree, S., Bowyer, K.: Predicting ethnicity and gender from iris texture. In: *IEEE International Conference on Technologies for Homeland Security (HST)*, (Nov 2011) 440–445
3. Thomas, V., Chawla, N., Bowyer, K., Flynn, P.: Learning to predict gender from iris images. In: *First IEEE International Conference on Biometrics: Theory, Applications, and Systems, BTAS 2007*. (Sept 2007) 1–5
4. Tapia, J., Perez, C.: Gender classification based on fusion of different spatial scale features selected by mutual information from histogram of LBP, Intensity, and Shape. *IEEE Transactions on Information Forensics and Security*, **8**(3) (2013) 488–499
5. He, Y., Feng, G., Hou, Y., Li, L., Micheli-Tzanakou, E.: Iris feature extraction method based on lbp and chunked encoding. In: *Seventh International Conference on Natural Computation (ICNC)*. Volume 3. (July 2011) 1663–1667
6. Yang, M.H., Moghaddam, B.: Gender classification using support vector machines. *Proc. Int Image Processing Conf* **2** (2000) 471–474
7. Makinen, E., Raisamo, R.: Evaluation of gender classification methods with automatically detected and aligned faces. *IEEE Transactions on Pattern Analysis and Machine Intelligence* **30**(3) (2008a) 541–547
8. Perez, C., Tapia, J., Estevez, P., Held, C.: Gender classification from face images using mutual information and feature fusion. *International Journal of Optomechatronics* **6**(1) (2012) 92–119
9. Bansal, A., Agarwal, R., Sharma, R.K.: SVM based gender classification using iris images. (Nov 2012) 425–429
10. Lyle, J., Miller, P., Pundlik, S., Woodard, D.: Soft biometric classification using periocular region features. In: *Fourth IEEE International Conference on Biometrics: Theory Applications and Systems (BTAS)*, 2010. (Sept 2010) 1–7

11. Merkow, J., Jou, B., Savvides, M.: An exploration of gender identification using only the periocular region. In: Fourth IEEE International Conference on Biometrics: Theory Applications and Systems (BTAS), 2010. (Sept 2010) 1–5
12. Peng, H., Long, F., Ding, C.: Feature selection based on mutual information criteria of max-dependency, max-relevance, and min-redundancy. *IEEE Transactions on Pattern Analysis and Machine Intelligence* **27**(8) (2005) 1226–1238
13. Liu, X., Bowyer, K., Flynn, P.: Experiments with an improved iris segmentation algorithm. In: Fourth IEEE Workshop on Automatic Identification Advanced Technologies. (Oct 2005) 118–123
14. Ojala, T., Pietikainen, M., Maenpaa, T.: Multiresolution gray-scale and rotation invariant texture classification with local binary patterns. *IEEE Transactions on Pattern Analysis and Machine Intelligence* **24**(7) (2002) 971–987
15. Lei, Z., Ahonen, T., Pietikainen, M., Li, S.Z.: Local frequency descriptor for low-resolution face recognition. In: FG. (2011) 161–166
16. Guo, Z., Zhang, L., Zhang, D.: Rotation invariant texture classification using lbp variance (lbpv) with global matching. *Pattern Recognition*. **43**(3) (March 2010) 706–719
17. Guo, Z., Zhang, D., Zhang, D.: A completed modeling of local binary pattern operator for texture classification. *IEEE Transactions on Image Processing*, **19**(6) (June 2010) 1657–1663
18. Zhou, H., Wang, R., Wang, C.: A novel extended local-binary-pattern operator for texture analysis. *Information Sciences* **178**(22) (2008) 4314 – 4325
19. Shan, C.: Learning local binary patterns for gender classification on real-world face images. *Pattern Recognition Letters* **33**(4) (2012) 431 – 437 *Intelligent Multimedia Interactivity*.
20. Daugman, J.: How iris recognition works. *IEEE Transactions on Circuits and Systems for Video Technology*, **14**(1) (Jan 2004) 21–30
21. Bowyer, K.W., Hollingsworth, K.: The best bits in an iris code. *IEEE Transactions on Pattern Analysis and Machine Intelligence* **31**(6) (2009) 1–1
22. Libor Masek, P.K.: Matlab source code for a biometric identification system based on iris patterns. The School of Computer Science and Software Engineering, The University of Western Australia. (2003)
23. Chang, C.C., Lin, C.J.: LIBSVM: A library for support vector machines. *ACM Transactions on Intelligent Systems and Technology* **2** (2011) 1–27